A Numerical Method to Analyze Unsteady Heat Transfer and Flow During Chilldown of a Cryogenic Transfer Line

Robert F. Colbert, Barry F. Battista, and Alok K. Majumdar
Sverdrup Technology, Huntsville, Alabama

David A. Shular and James W. Owen
Marshall Space Flight Center, Huntsville, Alabama

Abstract

The subject of this paper is a numerical method, devised to perform transient venting analyses and to describe the corresponding temperature response of a Cryogenic Transfer Line (CTL). In the present treatment, the CTL was regarded as a single control volume, into which a saturated liquid cryogen was introduced. Unsteady mass, momentum and energy conservation equations (i.e. for the liquid and vapor phases) were solved in conjunction with Vanderwaal's equation of state. A fully-implicit, successive substitution method was employed to solve the resulting coupled, non-linear equations. A corresponding FORTRAN code was developed to predict the pressure and temperature histories, within a CTL, for a proposed ground test facility at the Marshall Space Flight Center. This paper includes a description of the test article and procedure.

1.0 Introduction

To successfully perform on-orbit re-supply of cryogenic fluids, a complete understanding of the thermal and fluid dynamic transients associated with cooling the transfer systems must be achieved. This requirement is of paramount importance, given that extended missions will require re-supply. Affected missions/vehicles include (but are not necessarily limited to) manned Lunar/Mars missions, the Space Transfer Vehicle (STV), the Space Station Freedom (SSF), and the proposed super-fluid Helium users (e.g. Advanced X-Ray Astrophysics Facility and ASTROMAG).

Chill-down of a transfer line is a natural consequence of routine cryogenic fluid transfer. The primary objective is to quickly cool the line, so as to promote homogeneous liquid transfer and/or to continue an ongoing test. On-orbit re-supply places additional constraints on the chilldown process. The amount of cryogen used to cool the line must be minimized due to the high cost (per pound) of payloads transported to orbit. Total chilldown time must also be considered because the transfer operation must be performed such that the user spacecraft is not removed from service for an extended period of time.[1]

Early testing was performed in 1966 at the National Bureau of Standards (NBS).[2, 3] This test series was initiated to characterize the thermal response of two 3/4-inch-diameter, vacuum jacketed, copper transfer lines, using liquid hydrogen (LH2) and liquid nitrogen (LN2) Various inlet pressures and temperatures were investigated. Test results showed that pressure and flow surges occurred during the initial phase of CTL chill-down. In fact, maximum pressures were sometimes observed to exceed 40 atmospheres. Investigators hypothesized that these surges occurred when the temperature of incoming liquid exceeded the local saturation temperature, resulting in rapid boiling (or "flashing") and a rapid increase in the specific volume of the fluid. Expansion created a sharp rise in the local pressure resulting in backflow within the line. Cyclic pressure surges were expected as the liquid front proceeded toward the open end of the line and the temperature of the CTL wall approached that of the incoming fluid.

Predicting the transient pressure distribution and thermal response of a cryogenic transfer line was again investigated in connection with a program to construct a ground test bed facility at the

Marshall Space Flight Center (MSFC).[8] The facility was conceived to evaluate different design and operational procedures for a typical fluid transfer line (such as might be used to conduct an STV re-supply mission). The baseline system comprises a 100-foot stainless steel pipe and a large thermal mass, intended to simulate a fluid coupling. A thermal/flow analysis was performed by Martin Marietta Space Systems (MMSS) to determine the temperature and pressure transients that would occur during the chill-down process.[1] MMSS later developed a detailed mathematical model using the thermal network analyzer, SINDA85/FLUINT.[4]

In the present paper, attention is directed toward identifying and describing the physical processes that occur when a saturated cryogenic liquid is introduced to a relatively warm transfer line. The differential equations governing the ensuing events were constructed and a numerical algorithm was developed to solve these equations.[12] Pre-test predictions of the transient pressure and temperature distributions, within the proposed CTL, were obtained using a computer program that was constructed from the aforementioned numerical algorithm. A brief description of the test article and testing procedure is also included in the paper.

2.0 CTL Test Article Description and Testing Approach

The testing approach taken has been to construct a full-scale test article which would represent a fluid transfer line that might be used to link a propellant depot to a space transfer vehicle (STV). The front and top views of the MSFC Cryogenic Transfer Line Facility (CTL) are shown in Fig. 1 and 2, respectively.

To perform CTL testing, the Foam/MLI cryogenic storage tank (FMLI test article) will be connected to the transfer line and utilized as a receiver vessel. The thermal environment for the CTL/FMLI assembly will be established primarily through the use of GH_2/GHe injection with additional control provided by the FMLI heater shield assembly used and the vacuum chamber LN_2 cold walls. Internal line pressure will be controlled through the use of an ejector pump located in the vent system. Since the CTL is an orbital transfer system, the vacuum chamber will be required to obtain a vacuum in the 10^{-6} torr range.

An accurate characterization of the transfer line will require a record of CTL temperature and pressure responses along with LH_2 consumption and GH_2 venting. These measurements will be made with thermocouples, silicon diodes, pressure transducers and flow meters.

The overall length of the transfer line is approximately 120 feet. This length consists of a vertical section which extends from the vacuum chamber penetration up to the CTL support structure and a horizontal run which interfaces with the FMLI tank. All the tubing used consists of 321 stainless steel with a 2 inch O.D. and a wall thickness of 0.02 inch. Three different transfer line configurations will be tested as follows:

Transfer Line Configuration #1: This arrangement will consist of a stainless steel line without any internal coating or composite substances. This line will run from the chamber penetration to the valve box at the FMLI interface. This configuration will provide baseline performance data against which configurations 2 and 3 will be compared.

Transfer Line Configuration #2: For this arrangement the entire section of stainless steel will be replaced with a line, internally coated with Teflon, and tested in a similar manner to configuration #1.

Transfer Line Configuration #3: The last arrangement would consist of the same set up as presented in configuration 2 but with the addition of a short 11.5 foot composite section inserted near the valve box at the FMLI interface.

The entire support frame structure used to hold the transfer line and valve box is made of 304 stainless steel and attached directly to the top of the existing FMLI tank support structure. The line itself is seated in Teflon saddles which limit thermal conduction from the line to the support structure. The support structure used for FMLI testing will be shortened by removing the lower 84 inches tower section before the CTL is placed in the chamber. This lowering will allow for easier access to the test article elements. CTL instrumentation consisting of E-type thermocouples, silicon diodes and pressure transducers are scattered all along the transfer line.[8]

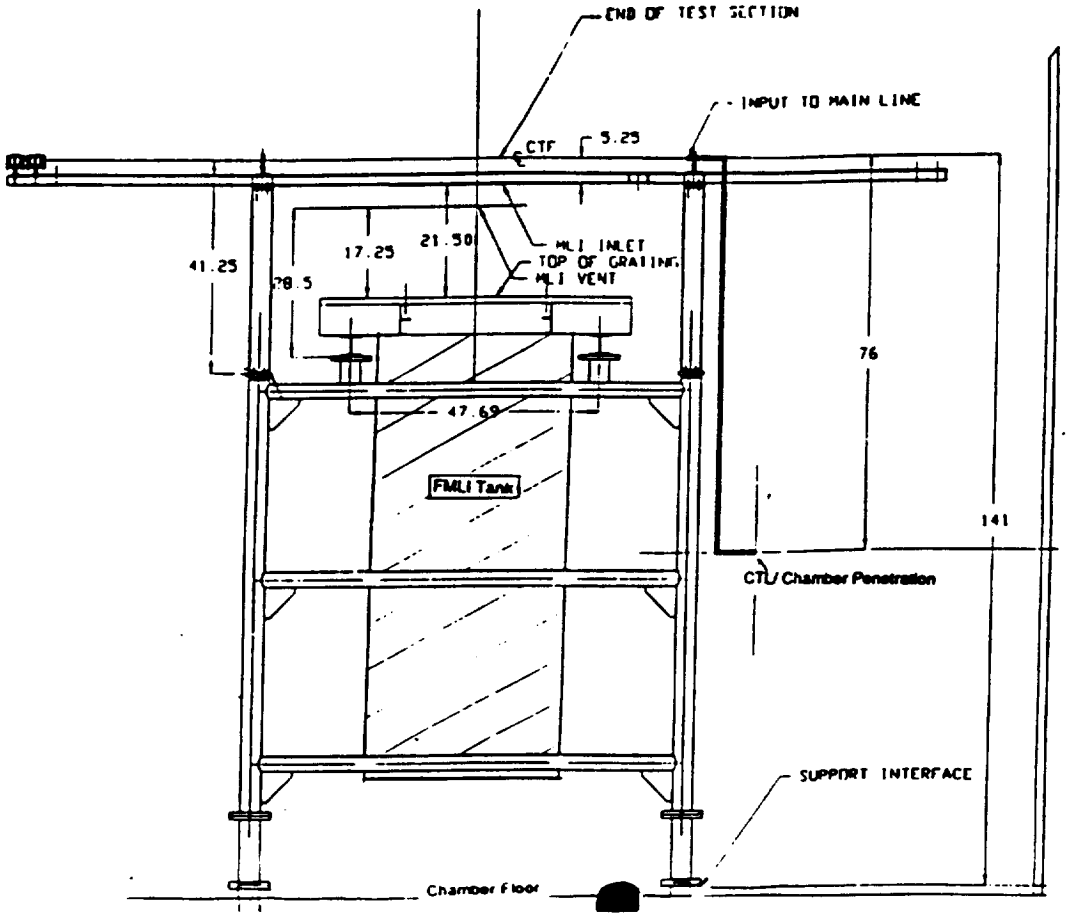

Figure 1. MSFC Cryogenic Transfer Line Facility (Front View)

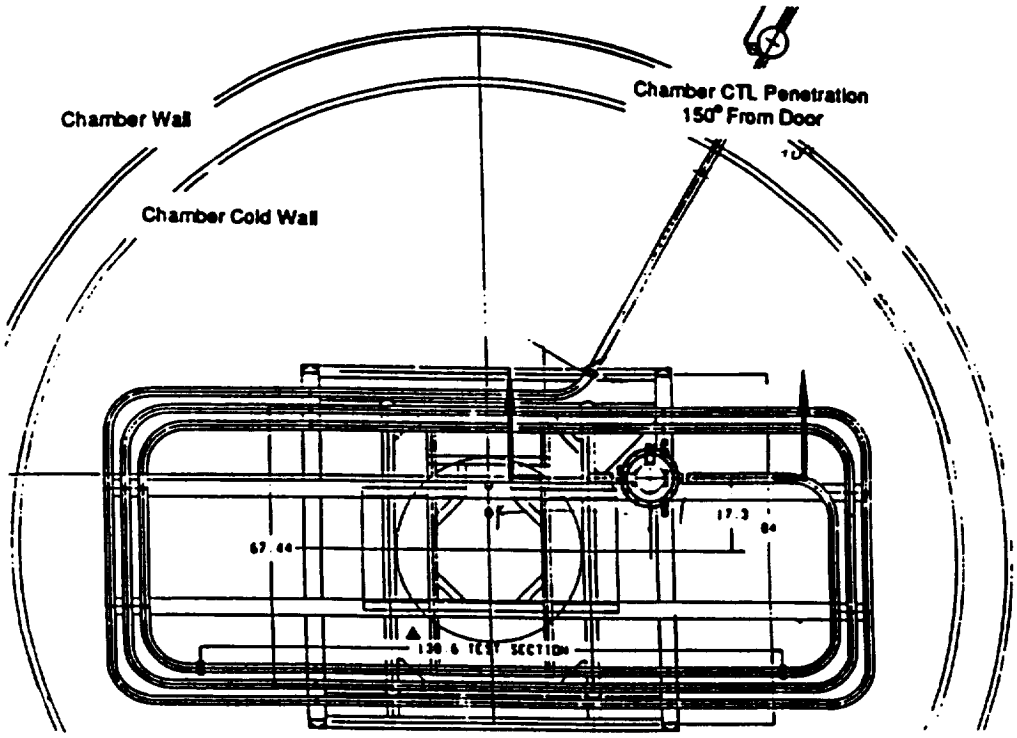

Figure 2. MSFC Cryogenic Transfer Line Facility (Top View)

3.0 Governing Equations

The technical approach discussed in this paper employed a "zero-dimensional" or lumped mass approach[5,6,7,12] developed at Sverdrup Technology, Inc. over the last three years. Due to inherent complexity associated with modeling transient flows accompanied by change of phase further development of the method was found necessary. These developments resulted into a new scheme that has been described below.

In developing a mathematical model of a physical system, it is helpful to ask three questions: 1) what are the physical processes occurring in the system?, 2) how can these physical processes be represented by a system of governing equations?, and 3) how can these system of equations be solved to predict the physical processes?

The physical processes which occur during chilldown of the cryogenic fluid transfer line system may be described as follows:

1) flow of cryogenic fluid (liquid) from the reservoir tank to the pipe line

2) heat transfer from the pipe wall to the flowing fluid, a mixture of liquid and vapor

3) a change of phase from liquid to vapor

4) flow of fluid (vapor) from the pipe line to the receiver tank

These four processes must be represented by a system of governing conservation equations for both mass and energy. Fig. 3 illustrates the mathematical model used to describe these processes occurring within the CTL.

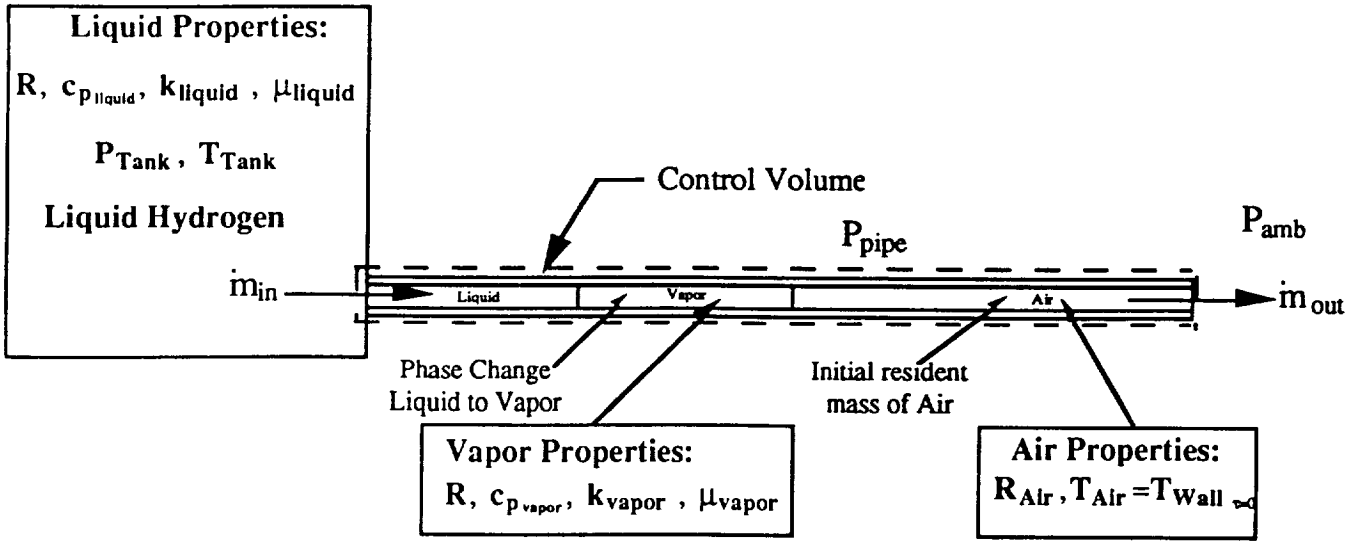

Figure 3. Mathematical Model for the MSFC Cryogenic Transfer Line Facility

3.1 Liquid Mass Flow Rate Equation

The first physical process is described by the mass flowrate of cryogenic fluid (liquid) entering the pipe (see Fig. 4) which is estimated from the Bernoulli equation

$$\dot{m}_{in} = C_D \rho_l A_{pipe} \sqrt{\frac{2 g_c 144 (P_{tank} - P_{pipe})}{\rho_l}} \qquad (1)$$

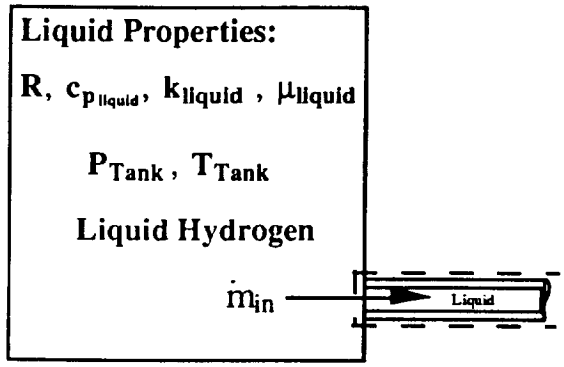

Figure 4. Schematic of CTL Pipe Entrance

where C_D is the discharge coefficient, ρ_l is the fluid (liquid) density, A_{pipe} is the cross-sectional area of the pipe, g_c is the conversion constant. The unsteady term in the Euler equation has been neglected.

The discharge coefficient, C_D, is given by

$$C_{D_{inlet}} = \frac{1}{\sqrt{\frac{fL_l}{D} + \frac{1 - c_c}{c_c^2}}} \tag{2}$$

where f is the friction factor, L_l is the liquid fluid length, D is the pipe diameter, and c_c is the coefficient of contraction.

3.2 Heat Transfer Rate

The second physical process is described by the rate of heat transfer from the pipe wall to the flowing fluid (see Fig. 5) which is given by

$$\dot{q} = h_{c_l} A_{s_l} (T_{wall} - T_{pipe}) + h_{c_v} A_{s_v} (T_{wall} - T_{pipe}) \tag{3}$$

where h_C is the forced convection heat transfer coefficient, A_S is the wetted surface area of the pipe for liquid and vapor regimes, T_{pipe} is the fluid temperature and T_{wall} is the wall temperature of the transfer line.

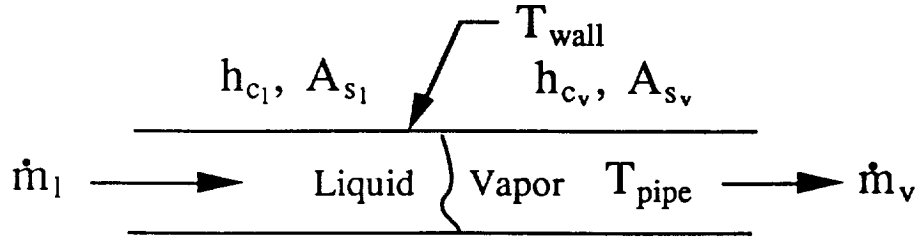

Figure 5. Schematic of CTL Fluid Interface

For fully developed turbulent flow in smooth tubes, the following relations for determining the forced convection heat transfer coefficient for both the liquid and vapor regimes is recommended by Dittus and Boelter, Ref.[6]

$$h_{c_l} = 0.0265 \frac{K_l}{D} \left(\frac{\rho_l u_l D}{\mu_l} \right)^{0.8} \left(\frac{c_{p_l} \mu_l}{K_l} \right)^{0.3} \tag{4}$$

and

$$h_{c_v} = 0.0265 \frac{K_v}{D} \left(\frac{\rho_v u_v D}{\mu_v} \right)^{0.8} \left(\frac{c_{p_v} \mu_v}{K_v} \right)^{0.3} \tag{5}$$

where K is the thermal conductivity of the fluid, u is the average velocity of the fluid, ρ is the density of the fluid, D is the pipe diameter, μ is the absolute viscosity of the fluid, and c_p is the specific heat at constant pressure (for the fluid); all properties are computed for the appropriate phases of the fluid (i.e., vapor or liquid).

3.3 Phase Change from Liquid to Vapor

The third physical process is a change of phase from liquid to vapor. Within the saturation dome (see Fig. 6) the rate of vapor being generated from the phase change is estimated by

$$\dot{m}_g = \frac{\dot{q}}{h_{fg}} \qquad (6)$$

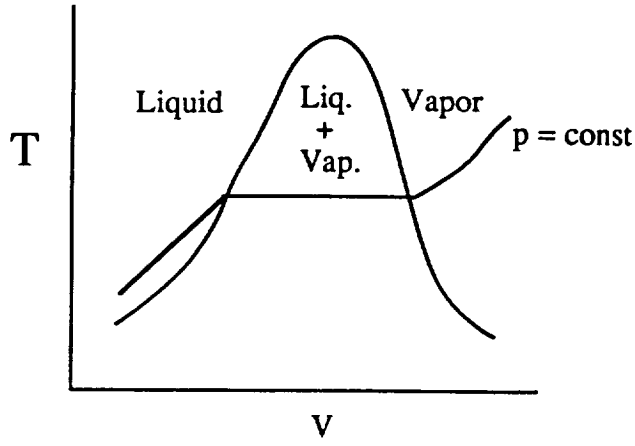

Figure 6. Schematic of Temperature-Volume Diagram

where $\dot{m}_g$ is the rate of vapor generated during the phase change, $\dot{q}$ is the rate of heat flow from the pipe wall to the flowing fluid, and h_{fg} is the latent heat of vaporization. The latent heat of vaporization, h_{fg}, may be estimated from the Clausius-Clapeyron equation

$$h_{fg} = T_{sat}(v_g - v_f)\frac{dP}{dT} \qquad (7)$$

where the saturation temperature, T_{sat}, and dP/dT are determined from an equation (Eq. 8) which describes the vapor-pressure curve for a pure substance (see Fig. 7),

$$\ln P = A + \frac{B}{T} + C\ln T + DT \qquad (8)$$

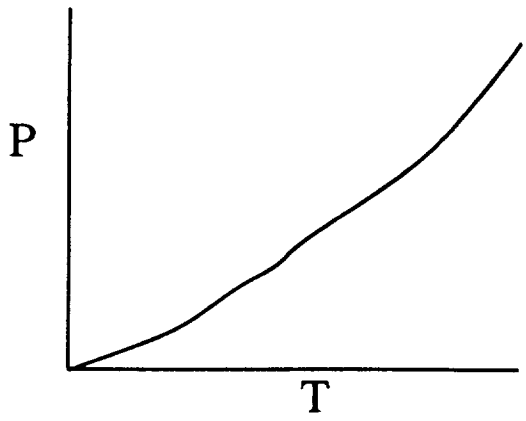

Figure 7. Schematic of Vapor-Pressure Curve for a Pure Substance

and the constants for Hydrogen are given by

A = 2.117096
B = -158.5594
C = 1.241988
D = 0.0119178

3.4 Vapor Mass Flow Rate

The last physical process is described by the mass flowrate of cryogenic fluid (vapor) leaving the pipe (see Fig. 8) which is estimated from the Bernoulli equation

$$\dot{m}_{out} = C_D \rho_v A_{pipe} \sqrt{\frac{2 g_c 144 (P_{pipe} - P_{amb})}{\rho_v}} \tag{9}$$

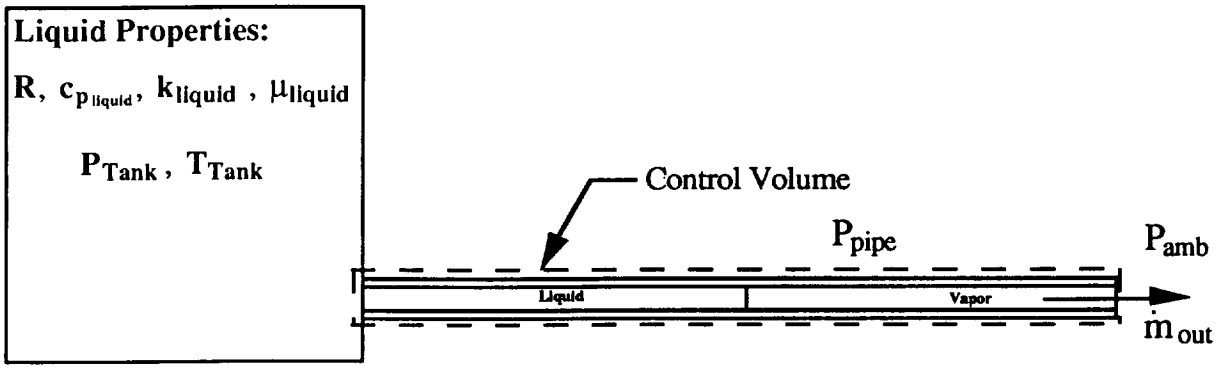

Figure 8. Schematic of CTL Pipe Exit

where C_D is the discharge coefficient, ρ_v is the fluid (vapor) density, A_{pipe} is the cross-sectional area of the pipe, g_c is the conversion constant. The unsteady term in the Euler equation has been neglected.

The discharge coefficient, C_D, is estimated by

$$C_{D_{outlet}} = \frac{1}{\sqrt{\frac{fL_g}{D} + N_{Bends}}} \tag{10}$$

where N_{Bends} is the number of bends in the pipe and L_g is the vapor fluid length.

3.5 Liquid Mass Conservation Equation

The next step is to integrate these physical processes into a set of governing conservation equations for both the mass and energy.

The liquid mass conservation equation in discretized form is given by

$$m_{l_{\tau+\Delta\tau}} = m_{l_\tau} + \dot{m}_l \Delta\tau - \dot{m}_g \Delta\tau \tag{11}$$

where m_l is the resident mass of liquid at the current and previous time step, $\dot{m}_l$ is the mass flowrate of liquid entering the pipe, $\dot{m}_g$ is the rate of vapor mass being generated as a result of the phase change, and τ is the time.

3.6 Vapor Mass Conservation Equation

Likewise, the vapor mass conservation equation in discretized form is given by

$$m_{v_{\tau+\Delta\tau}} = m_{v_\tau} + \dot{m}_g\Delta\tau - \dot{m}_v\Delta\tau \tag{12}$$

where m_v is the resident mass of vapor at the current and previous time step, $\dot{m}_v$ is the mass flowrate of vapor leaving the pipe, and $\dot{m}_g$ is the rate of vapor mass being generated as a result of heating.

3.7 Total Mass Conservation Equation

By adding both sides of the liquid and vapor mass conservation equations (Eq. 11 and 12) and then substituting the left hand side of Eq. 13 and 14, the following result (Eq. 15) is obtained

$$m_{\tau+\Delta\tau} = m_{l_{\tau+\Delta\tau}} + m_{v_{\tau+\Delta\tau}} \tag{13}$$

$$m_\tau = m_{l_\tau} + m_{v_\tau} \tag{14}$$

The complete mass conservation equation in discretized form may be expressed as

$$m_{\tau+\Delta\tau} = m_\tau + \dot{m}_l\Delta\tau - \dot{m}_v\Delta\tau \tag{15}$$

3.8 Pressure Equation

A pressure equation is next derived from the mass conservation equation. The purpose of this derivation is to relate pressure (in the flow equation) to a thermodynamic equation of state.

The complete mass conservation equation (Eq. 15) can be rewritten as

$$\dot{m}_{in} = \frac{dm}{d\tau} + \dot{m}_{out} \tag{16}$$

where the mass flowrates are given in Eq. 1 and 9.

The time rate of change of the resident mass in discretized form is given by

$$\frac{dm}{d\tau} = \frac{m_{\tau+\Delta\tau} - m_\tau}{\Delta\tau} \tag{17}$$

Assuming the ideal gas law to be applicable, the resident fluid mass in the pipe may be written as

$$m_{\tau+\Delta\tau} = \frac{P_{pipe_{\tau+\Delta\tau}} V_{v_{\tau+\Delta\tau}}}{Z_{v_{\tau+\Delta\tau}} R T_{pipe_{\tau+\Delta\tau}}} + \frac{P_{pipe_{\tau+\Delta\tau}} V_{l_{\tau+\Delta\tau}}}{Z_{l_{\tau+\Delta\tau}} R T_{pipe_{\tau+\Delta\tau}}} + \frac{P_{pipe_{\tau+\Delta\tau}} V_{air_{\tau+\Delta\tau}}}{R_{air} T_{air_{\tau+\Delta\tau}}} \tag{18}$$

$$m_\tau = \frac{P_{pipe_\tau} V_{v_\tau}}{Z_{v_\tau} R T_{pipe_\tau}} + \frac{P_{pipe_\tau} V_{l_\tau}}{Z_{l_\tau} R T_{pipe_\tau}} + \frac{P_{pipe_\tau} V_{air_\tau}}{R_{air} T_{air_\tau}} \tag{19}$$

where Z is the compressibility factor, R is the gas constant for hydrogen, R_{air} is the gas constant for air, and V is the volume of the fluid, a mixture of liquid, vapor, and air.

Following the substitutions of Eq. 1, 9 and 17 through 19 into the mass conservation equation, Eq. 16 can then be rewritten as

$$\frac{(C_D \rho_l A_{pipe})_{inlet}}{\sqrt{144(P_{tank} - P_{pipe_{\tau+\Delta\tau}})}} \sqrt{\frac{2g_c}{\rho_l}} (P_{tank} - P_{pipe_{\tau+\Delta\tau}}) = \frac{P_{pipe_{\tau+\Delta\tau}} V_{v_{\tau+\Delta\tau}}}{\Delta\tau Z_{v_{\tau+\Delta\tau}} R T_{pipe_{\tau+\Delta\tau}}} + \frac{P_{pipe_{\tau+\Delta\tau}} V_{l_{\tau+\Delta\tau}}}{\Delta\tau Z_{l_{\tau+\Delta\tau}} R T_{pipe_{\tau+\Delta\tau}}} + \frac{P_{pipe_{\tau+\Delta\tau}} V_{air}}{\Delta\tau R_{air} T_{air}}$$

$$- \frac{P_{pipe_\tau} V_{v_\tau}}{\Delta\tau Z_{v_\tau} R T_{pipe_\tau}} - \frac{P_{pipe_\tau} V_{l_\tau}}{\Delta\tau Z_{l_\tau} R T_{pipe_\tau}} - \frac{P_{pipe_\tau} V_{air}}{\Delta\tau R_{air} T_{air}} + \frac{(C_D \rho_v A_{pipe})_{outlet}}{\sqrt{144(P_{pipe_\tau} - P_{amb})}} \sqrt{\frac{2g_c}{\rho_v}} (P_{pipe_\tau} - P_{amb}) \tag{20}$$

The mass conservation (Eq. 16) is now expressed in terms of pressure. Equation 20 is also expressed in linearized form and is solved using an iterative method.

The above pressure equation can be expressed in a conservative form as follows

$$DP_{pipe_{\tau+\Delta\tau}} = AP_{tank} + BP_{amb} + CP_{pipe_\tau} \tag{21}$$

where the coefficients are given by

$$A = \frac{(C_D \rho_l A_{pipe})_{inlet}}{\sqrt{144(P_{tank} - P_{pipe})}} \sqrt{\frac{2g_c}{\rho_l}} \tag{22}$$

$$B = \frac{(C_{D_v} \rho_v A_{pipe})_{outlet}}{\sqrt{144(P_{pipe_{\tau+\Delta\tau}} - P_{amb})}} \sqrt{\frac{2g_c}{\rho_v}} \quad \text{or} \quad \frac{(C_{D_{air}} \rho_{air} A_{pipe})_{outlet}}{\sqrt{144(P_{pipe_{\tau+\Delta\tau}} - P_{amb})}} \sqrt{\frac{2g_c}{\rho_{air}}} \tag{23}$$

$$C = \frac{V_{v_\tau}}{\Delta\tau R T_{pipe_\tau}} + \frac{V_{l_\tau}}{\Delta\tau Z_\tau R T_{pipe_\tau}} + \frac{V_{air_\tau}}{\Delta\tau R_{air} T_{air}} \tag{24}$$

$$D = A + B + \frac{V_{v_{\tau+\Delta\tau}}}{\Delta\tau R T_{pipe_{\tau+\Delta\tau}}} + \frac{V_{l_{\tau+\Delta\tau}}}{\Delta\tau Z_{\tau+\Delta\tau} R T_{pipe_{\tau+\Delta\tau}}} + \frac{V_{air_{\tau+\Delta\tau}}}{\Delta\tau R_{air} T_{air}} \tag{25}$$

Equation 21 is non-linear since the coefficients A and B are functions of P_{tank} and P_{amb}, respectively. It may be noted in Eq. 23 that there is no flow of hydrogen vapor exiting the pipe until the air has been displaced.

Let us now address the question of coupling between heat transfer and fluid flow. In Eq. 21, the heat transfer effect is conveyed through the coefficient C (see Eq. 24). This coefficient accounts for the contributions to pressure of both the liquid, vapor and air if present. Furthermore, if the temperature drops quickly, the corresponding decrease in the line pressure gives rise to a transient effect that is predicted through this coefficient. It may also be noted that by setting the constant C

equal to zero results in the steady-state solution because the transient nature occurs through the energy equation.

3.9 Energy Conservation Equation

The next step in the determining a set of governing conservation equations is to derive the energy conservation equation. For the CTL there are two energy equations, one for the fluid in the pipe and one for the pipe wall itself (see Fig. 9 and 10).

An applicable form of the energy conservation equation for the fluid in the pipe is given by

$$\dot{m}_{in}h_{in} + \dot{q} = \dot{m}_{out}h_{out} + \frac{d}{d\tau}\left(mu + \frac{m\bar{V}^2}{2}\right) \tag{26}$$

In discretized form Eq. 26 may be rewritten as follows

$$m_{pipe_{\tau+\Delta\tau}}u_{pipe_{\tau+\Delta\tau}} = m_{pipe_\tau}u_{pipe_\tau} + (\dot{m}_{in}h_{in} + \dot{q} - \dot{m}_{out}h_{out})\Delta\tau \tag{27}$$

It is noted that the time rate of change of kinetic energy, $\frac{d}{d\tau}\left(\frac{m\bar{V}^2}{2}\right)$, has been neglected. This assumption would not contribute to a significant error.

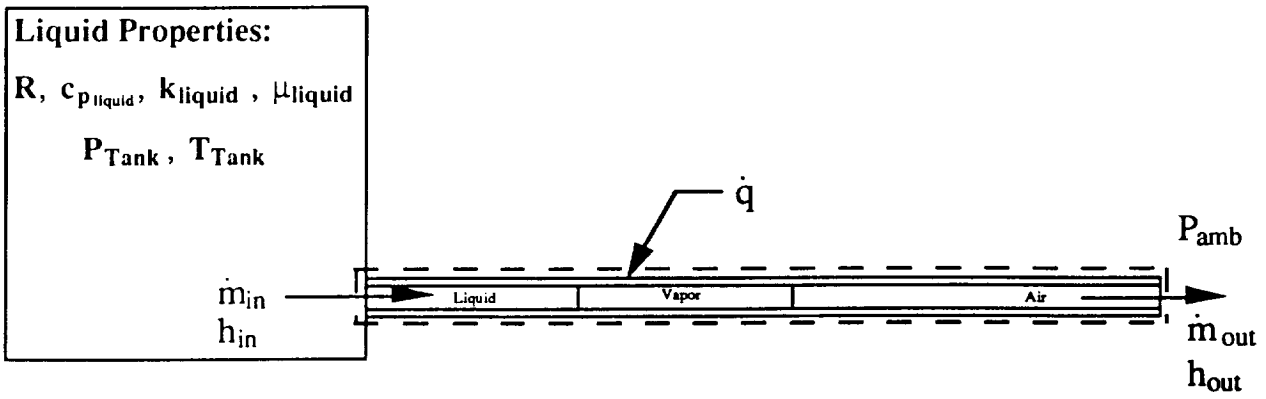

Figure 9. Schematic of CTL Illustrating the Heat Flowrate for the Fluid

For the CTL pipe wall, the energy equation may be expressed as

$$\frac{d}{d\tau}\left(m_{pipe}c_{p_{pipe}}T_{wall}\right) = -\dot{q} \tag{28}$$

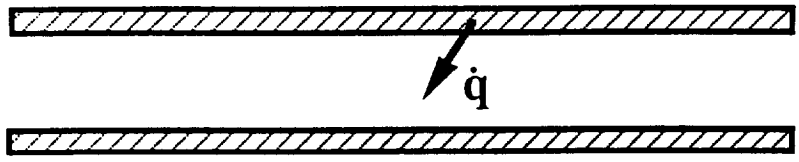

Figure 10. Schematic of CTL Illustrating Heat Flow from Pipe Wall to Fluid

where $\dot{q}$ is the rate of heat transfer from the pipe wall to the flowing fluid; m_{pipe} is the mass of the CTL (or pipe); $c_{p_{pipe}}$ is the specific heat of the pipe; and τ is the time. The pipe wall material is 321-stainless steel and hydrogen is the working fluid.

The wall temperature, T_{wall}, is calculated by rearranging Eq. (28) in discretized form

$$T_{wall_{\tau+\Delta\tau}} = T_{wall_{\tau}} - \frac{\dot{q}\Delta\tau}{m_{pipe}c_{p_{pipe}}} \tag{29}$$

3.10 Equation of State

The resident mass of liquid and vapor may be determined by the equation of state with the addition of an appropriate compressibility factor.

The liquid mass may be estimated by

$$m_{l_{\tau+\Delta\tau}} = \frac{P_{pipe_{\tau+\Delta\tau}} V_{l_{\tau+\Delta\tau}}}{Z_{l_{\tau+\Delta\tau}} R T_{pipe_{\tau+\Delta\tau}}} \tag{30}$$

The vapor mass may be estimated by

$$m_{v_{\tau+\Delta\tau}} = \frac{P_{pipe_{\tau+\Delta\tau}} V_{v_{\tau+\Delta\tau}}}{Z_{v_{\tau+\Delta\tau}} R T_{pipe_{\tau+\Delta\tau}}} \tag{31}$$

For an ideal fluid, the compressibility factor is given by $Z = \frac{Pv}{RT}$. For a real fluid, Z_l and Z_v may be expressed by the Van der Waal Equation given by

$$AZ^3 + BZ^2 + CZ + D = 0 \tag{32}$$

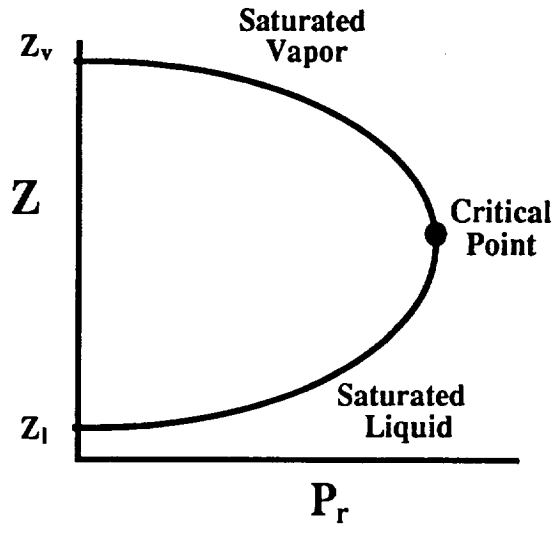

Figure 11. Schematic of Compressibility Chart for a Pure Substance

The Van der Waal Equation is a cubic polynomial with two real roots Z_l and Z_v and an imaginary or complex root. The compressibility factor for Z_v has been assumed to be 1. The liquid compressibility factor, however, is calculated using the bisection method in determining the roots of the equation. The constants are determined from the following expressions:

$$A=1 \tag{33}$$

$$B = -\left(\frac{P_r}{8T_r} + 1\right) \tag{34}$$

$$C = \left(\frac{27P_r}{64T_r^2}\right) \tag{35}$$

$$D = -\left(\frac{27P_r^2}{512T_r^3}\right) \tag{36}$$

$$P_r = \frac{P_{pipe}}{P_{crit}} \tag{37}$$

$$T_r = \frac{T_{pipe}}{T_{crit}} \tag{38}$$

3.11 Pipe Fluid Temperature

The fluid temperature in the CTL is evaluated in accordance with the following procedure:

1. For the given fluid pressure, P_{pipe}, calculate the saturated internal energies for the liquid, u_f, and vapor, u_g.

2. Compare internal energy of the fluid within CTL, u_{pipe}, with the saturated internal energies for the liquid, u_f, and vapor, u_g.

$$\text{If } u_{pipe} < u_f;\ T_{pipe} = T_{sat} + \frac{(u - u_f)}{c_{v_l}} \tag{39}$$

$$\text{If } u_f \le u_{pipe} \le u_g;\ T_{pipe} = T_{sat}(P_{pipe}) \tag{40}$$

$$\text{If } u_{pipe} > u_g;\ T_{pipe} = T_{sat} + \frac{(u - u_g)}{c_{v_g}} \tag{41}$$

where c_v is the specific heat at constant volume for liquid and the vapor.

4.0 Numerical Solution Method

The differential equations described in the previous section has been solved by an iterative, fully implicit method. The calculation procedure comprises of the following steps (as illustrated in Fig. 12):

1. Initially the line contains Air at a ambient pressure. At time $\tau = 0$, $P_{pipe} = P_{amb}$ and $T_{pipe} = T_{amb}$.

2. Begin new time $\tau = \tau + \Delta\tau$

3. Calculate mass of liquid and vapor from mass conservation equations, Eq. 11 and 12.

4. Calculate P_{pipe} from pressure equation (Eq. 21).

5. Calculate internal energy of the working fluid from energy equation (Eq. 27).

6. Calculate wall temperature from energy equation for pipe wall (Eq. 29).

7. Calculate thermodynamic state properties from various thermodynamic property relationships.

8. Calculate working fluid temperature in pipe, T_{pipe}, from Eq. 39 through 41.

9. Calculate mass and energy percent error in the CTL at the beginning and at the end of each iteration given by

$$\Delta m = m_{old} - m_{new} \quad \text{and} \quad \Delta u = u_{old} - u_{new}$$

$$\text{Error} = \frac{|\Delta m|}{m_{old}} \quad \text{and} \quad \text{Error} = \frac{|\Delta u|}{u_{old}}$$

10. Repeat steps 3 to 9 until convergence is satisfied.

11. Move to a new time (step 2) and all subsequent steps are repeated until end of time or when the wall temperature equals the fluid temperature is reached.

Typical run times are between 3 to 6 minutes in a 486-based PC. Average number of iterations per time step (time step = 0.002 sec.) for the mass and energy loops are between 5 and 13, respectively. The convergence criterion for both the mass and energy loops was set at 1.0E-05. Mass and energy underrelaxation constants were arbitrarily set at 0.5. As of this writing their has been no attempt to perform an optimization study to obtain the best set of solution control parameters for an optimized solution.

5.0 Analysis Results

Predictions of the time-dependent pressure, temperature, resident mass, heat transfer coefficient, and (thermodynamic) quality are presented for various combinations of the tank pressure, exit pressure, and initial CTL wall temperature.[12]

Figure 13 depicts the pressure history for a supply (tank) pressure of 25 psia, an exit pressure of 5 psia, and an initial line wall temperature of 300 R. The plot shows a pressure spike of 225 psia, occuring at 0.15 seconds, followed by a steady pressure of 25 psia (through 4.6 seconds); after 4.6 seconds, the pressure gradually approached the exit value of 5 psia. A pressure fluctuation at approximately 4.2 seconds was attributed to the change in fluid conditions between the superheated and saturated regimes (as evidenced by the quality history). The CTL chill-down time was 5.8 seconds.

Figure 14 shows the predicted temperature history of the CTL wall and the fluid in the pipe. Here again, the CTL wall temperature was initially 300 R and decreased to the saturation temperature (i.e. 30 R) in 5.8 seconds. The fluid temperature rose to a maximum of 215 R, followed by an eventual decrease to 30 R. The fluid temperature instability stemmed from a difficulty associated with calculating fluid properties near the critical point.

Figure 15 gives the respective mass histories of the liquid and vapor phases, within the CTL. The mass of vapor initially peaked at 0.8 lbm (at 0.16 seconds) and later droped to 0.20 lbm (at 0.40 seconds). A gradual increase occured thereafter, followed by a monotonic decrease to zero, as vapor was ultimately replaced by a homogeneous liquid phase at 5.2 seconds. The liquid mass rose to 0.6 lbm (at 0.10 seconds) and then fell to zero; this phenomenon was attributed to the sharp

pressure rise (i.e. to a value exceeding the tank pressure) which tended to force the liquid column back into the supply tank. The liquid mass remained at zero until saturation conditions were again attained at 4.2 seconds. After 4.2 seconds, the predicted liquid mass began to rise. In general, the liquid mass continues to increase until the temperature of the CTL wall reaches the saturation temperature of the fluid (for known tank pressure) or until the liquid column reaches the open end of the pipe.

Figure 16 shows the heat transfer coefficient as a fuction of the time elapsed following introduction of fluid into the CTL. This plot suggests a rapid rise and a subsequent peak near 0.50 BTU/ft^2-R; the maximum value coincides with the reported pressure spike. The heat transfer coefficient undergoes a marked increase begining at approximately 4.6 seconds. This behavior is attributed to a concurrent increase in the mass flowrate of the liquid phase.

Finally, Figure 17 depicts the relationship between (thermodynamic) quality and the time elapsed from the start of fluid flow. This plot indicates that fluid conditions were initially saturated but that the quality increased as the fluid approached the superheated state. Saturated conditions were again attained at 4.2 seconds and a subsequent decrease in the quality was noted, up to the time at which the CTL wall temperature reached T_{sat}.

6.0 Conclusions

An original approach was developed and applied to predict unsteady heat transfer and fluid flow, within a cryogenic transfer line, during the cooling process. This method was used to estimate the chill-down time, as well as the pressure and temperature histories, for a CTL of known length and wall thickness. Numerical results appear plausible and support limited experimental data; however, validation of the methodology requires a direct comparison of transient predictions with a comprehensive body of test data (which is not yet available). The present work provides a foundation for the development of progressively more complex models involving one and two-dimensional representations of the CTL and/or intermixed two-phase flow.

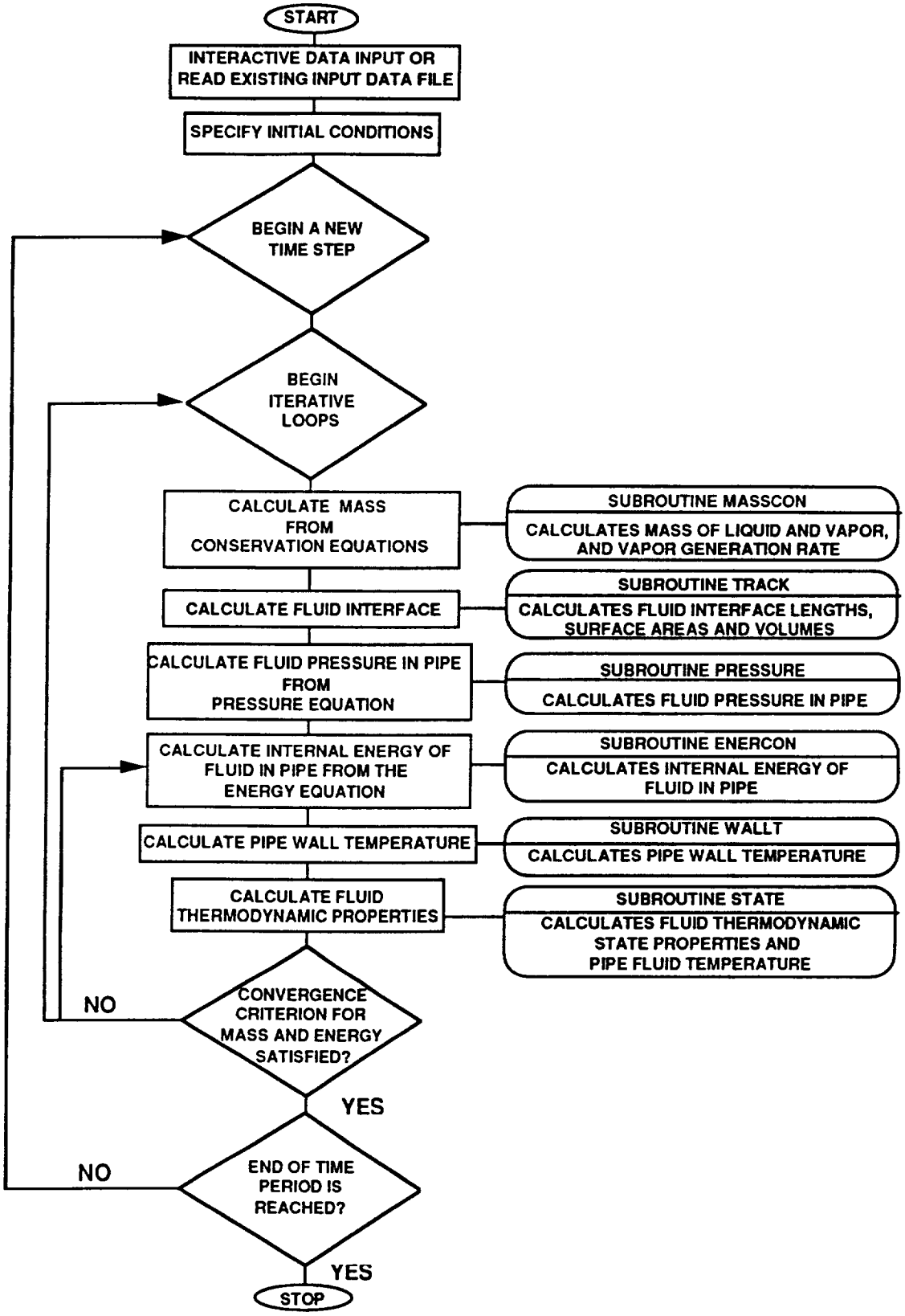

Figure 12. Flow Diagram of the CTLOD Fortran Code

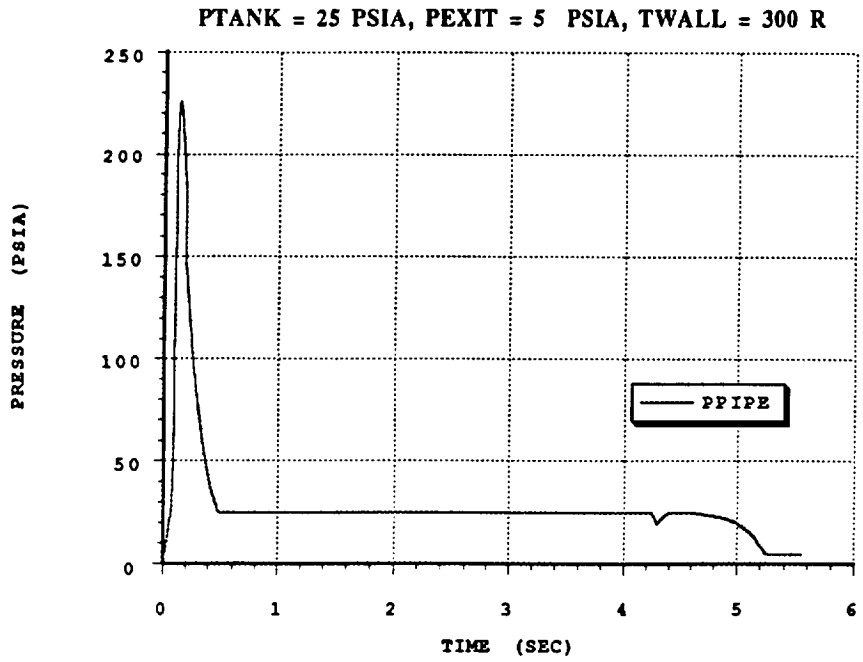

Figure 13. Line Pressure History with Saturated Liquid Hydrogen at a Driving Pressure of 25 psia, Exit Pressure of 5 psia, Twall of 300R.

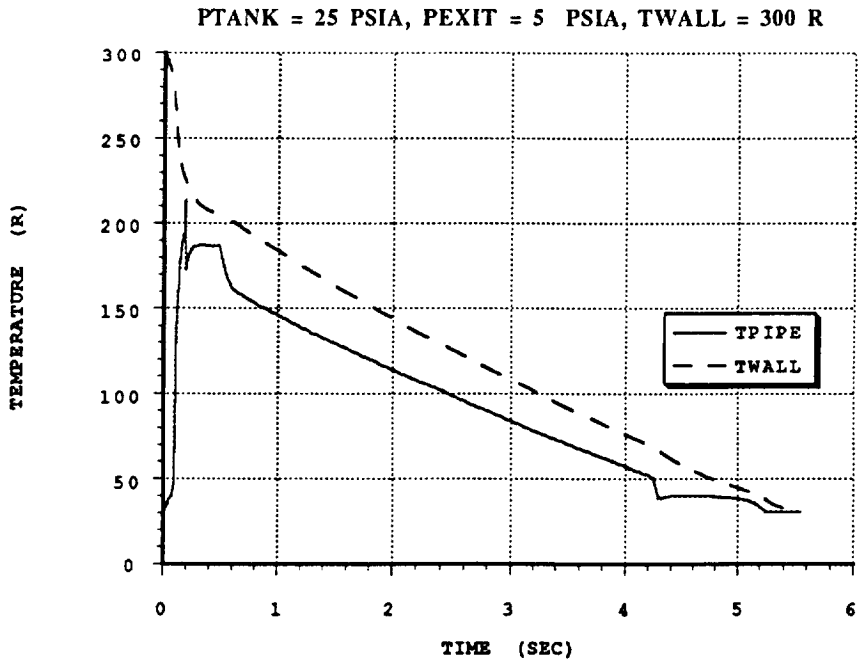

Figure 14. Line Temperature History with Saturated Liquid Hydrogen at a Driving Pressure of 25 psia, Exit Pressure of 5 psia, Twall of 300R.

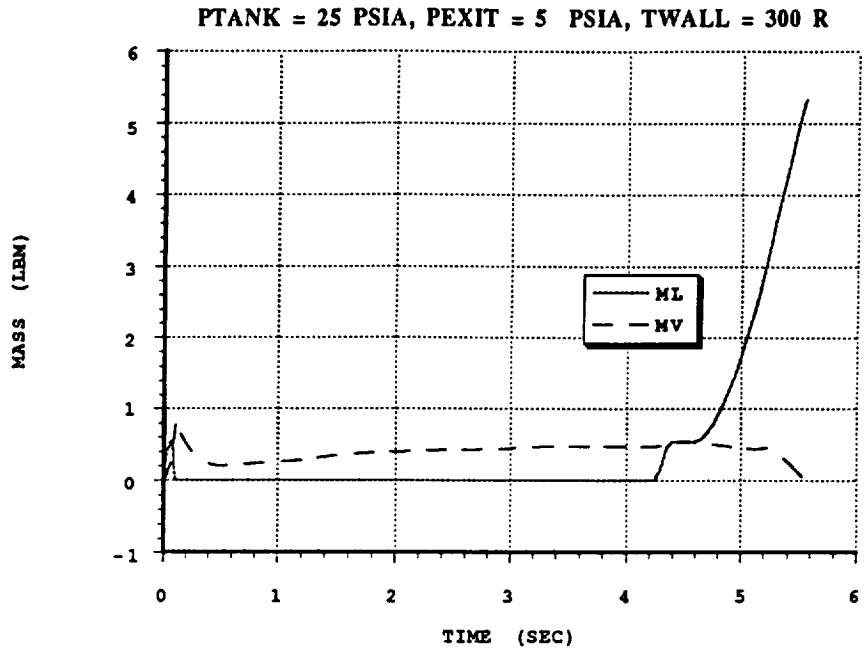

Figure 15. Line Mass History with Saturated Liquid Hydrogen at a Driving Pressure of 25 psia, Exit Pressure of 5 psia, Twall of 300R.

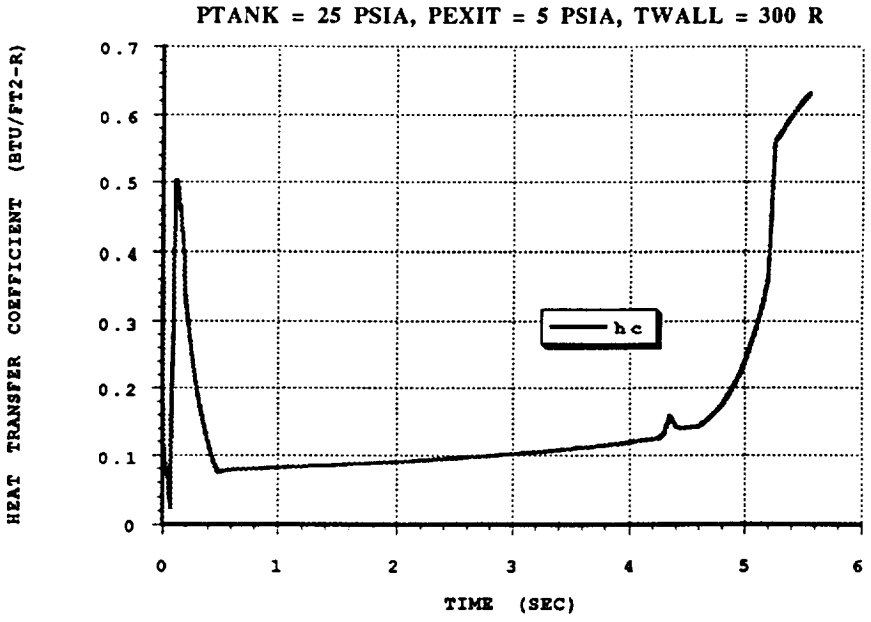

Figure 16. Line Heat Transfer Coefficient History with Saturated Liquid Hydrogen at a Driving Pressure of 25 psia, Exit Pressure of 5 psia, Twall of 300R.

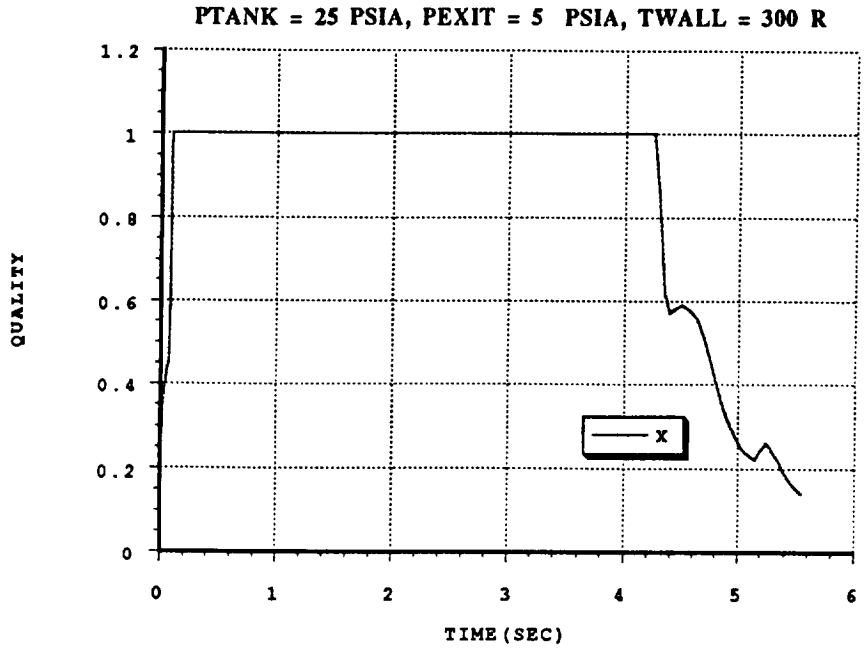

Figure 17. Line Fluid Quality History with Saturated Liquid Hydrogen at a Driving Pressure of 25 psia, Exit Pressure of 5 psia, Twall of 300R.

7.0 References

1. Martin, Tim, "Transient Analysis of Chilldown in a Cryogenic Transfer Line", AIAA 90-2374, 26th Joint Propulsion Conference, July, 1990.

2. Brennan, J.A., Brentari, E.G., Smith, R. V., Steward, W.G., " Cooldown of Cryogenic Transfer Lines - An Experimental Report", NBS Report No.9264, November 1966.

3. Steward, W.G., Smith, R.V., Brennan, J. A., "Cooldown Transients in Cryogenic Transfer Lines", Advances in Cryogenic Engineering, Vol. 15, 1970.

4. Cullimore, B.A., Goble, R.G., Jensen, C.L., Ring, S. G., "Systems Improved Numerical Differencing Analyzer - 1985 Version with Fluid Integrator (SINDA'85/FLUINT) User's Manual", Revision 3, Ver. 2.2, Contract # NAS9-17448, TR-86-594, September 1988.

5. Colbert, Robert, Bukkapatnam, Srinivas, Majumdar, Alok, "A Computer Program to Perform Thermodynamic and Flow Analysis During Pressurization and Depressurization of Connected Tubes (TACT), Sverdrup Technology, Inc., MSFC Group, March 1990, TN-SvT, MD5.1/90-001.

6. Colbert, Robert, Ghaffarian, Benny, Majumdar, Alok, "A Computer Program to Perform Flow and Thermal Analysis During Pressurization of the 70-LB Solid Rocket Test Motor (FLAP), Sverdrup Technology, Inc., MSFC Group, December 1990, TN-SvT-MD5.1/ 90-006.

7. Battista, Barry, Bukkapatnam, Srinivas, Majumdar, Alok, "CGF Loss of Coolant Analysis", Sverdrup Technology, Inc., MSFC Group, March 18, 1991.

8. Martin, J., "Test Plan MSFC Cryogenic Transfer Line (CTL) Ground Test Bed Facility", April 1992.

9. Dittus, F. W. and L.M.K. Boelter; University of California (Berkeley) Pub. Eng., Vol. 2, P. 443, 1930.

10. Van Wylen, Gordon J. and Sonntag, Richard E., "Fundamentals of Classical Thermodynamics", 2nd Edition, P. 406.

11. Streeter, Victor, Wylie, Benjamin, "Fluid Mechanics", Seventh Edition, 1979

12. Colbert, Robert F., Battista, Barry F., Majumdar, Alok K., "A Computer Program to Perform Flow and Thermal Analysis for Chilldown in a Cryogenic Transfer Line", Sverdrup Technology, Inc., MSFC Group, June 1992, Contract # NAS8-37814, Report # 651-008-92-002